Hybrid-duplex communications for multi-UAV networks : an outage probability analysis

Tan, Ernest Zheng Hui; Madhukumar, A. S.; Sirigina, Rajendra Prasad; Krishna, Anoop Kumar

2019

Tan, E. Z. H., Madhukumar, A. S., Sirigina, R. P. & Krishna, A. K. (2019). Hybrid-duplex communications for multi-UAV networks : an outage probability analysis. IEEE Communications Letters, 23(10), 1831-1835. doi:10.1109/LCOMM.2019.2929392

https://hdl.handle.net/10356/144697

https://doi.org/10.1109/LCOMM.2019.2929392

Hybrid-Duplex Communications for Multi-UAV Networks: An Outage Probability Analysis

Tan Zheng Hui Ernest, A S Madhukumar, Rajendra Prasad Sirigina, and Anoop Kumar Krishna

***Abstract*—In this work, the outage probability of an unmanned aerial vehicle (UAV) network with hybrid-duplex (HBD) UAV communications is investigated in a stochastic geometry framework. We demonstrate that the HBD UAV communication system (HBD-UCS) can concurrently support more UAVs while achieving higher reliability than the half-duplex (HD) UCS (HD-UCS). Specifically, at low transmit power regimes, it is shown that the HBD-UCS attains lower uplink and downlink outage probability than an HD-UCS, even as the UAV operating altitude is increased.**

***Index Terms*—Unmanned Aerial Vehicle, Full-Duplex, Hybrid-Duplex, Rician Fading, Stochastic Geometry.**

I. Introduction

Hybrid-duplex (HBD) systems have been recently investigated to address spectrum scarcity in both manned and unmanned aerial vehicle (UAV) communications [1], [2]. For HBD UAV communication systems (UCSs), i.e., HBD-UCSs, UAVs with legacy half-duplex (HD) UCSs, i.e., HD-UCSs, can simultaneously communicate with full-duplex (FD) ground stations (GSs) on the same spectrum. However, residual self-interference (SI) due to carrier phase noise and imperfect SI channel estimation [3], and interference between UAVs, i.e., inter-UAV interference, are some of the main impediments in the HBD systems [1], [2], [4]. In spite of the associated limitations, research interest in related FD terrestrial systems has been growing in the literature. Yet, the obtained conclusions may not be fully applicable for UAV communications largely due to significant differences in channel models [1], [5] and spatial location modeling [5], [6] between terrestrial and UAV networks. [1] With these considerations in mind, a multi-UAV network with HBD-UCS is investigated in this work under a stochastic geometry framework. The remainder of this paper is organized as follows. The system model is introduced in Section II. Outage probability expressions are presented in Section III, with numerical results discussed in Section IV before the conclusion of the paper in Section V.

Tan Zheng Hui Ernest is with the School of Computer Science and Engineering, Nanyang Technological University, Singapore e-mail: (tanz0119@e.ntu.edu.sg).

A S Madhukumar is with the School of Computer Science and Engineering, Nanyang Technological University, Singapore e-mail: (asmadhukumar@ntu.edu.sg).

Rajendra Prasad Sirigina is with the School of Computer Science and Engineering, Nanyang Technological University, Singapore e-mail: (raje0015@ntu.edu.sg).

Anoop Kumar Krishna is with Airbus Singapore Pte Ltd, Singapore e-mail: (anoopkumar.krishna@airbus.com).

[1]Rayleigh fading channels have been commonly assumed for terrestrial networks. However, the Rician fading model is more suitable for aerial communications [1], [2], [7]. Likewise, the Poisson point process (PPP) is commonly used for terrestrial networks. However, the binomial point process (BPP) is more suitable for the modeling of UAV spatial locations [5], [6].

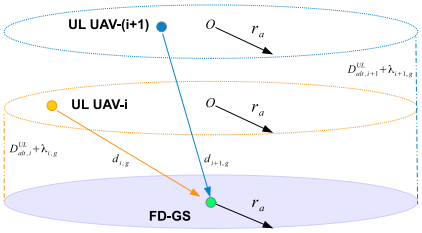

Fig. 1. An illustration of the UL UAV spatial locations. The spatial location of DL UAV-1 is described in the same fashion.

II. System Model

We consider an HBD-UCS with N_{UL} HD uplink (UL) UAVs and one HD downlink (DL) UAV communicating with a FD-GS in a suburban environment. In particular, the FD-GS receives uplink data from the N_{UL} UL UAVs while simultaneously transmitting downlink data to the DL UAV. Furthermore, inter-UAV interference between the UL and DL UAVs is unavoidable due to the nature of HBD transmissions [1], [2]. Thus, a successive interference cancellation (SIC) detector is considered at the DL UAV, with SI mitigation assumed at the FD-GS in this paper. To account for the spatial deployment of UAVs, a BPP assumption is considered [5], [6], with $D^{UL}_{alt,i}$ denoting the altitude of UL UAV-i and $D^{DL}_{alt,1}$ denoting the altitude of the DL UAV. Rician fading channels are also assumed to appropriately model the propagation characteristics of the suburban environment in UAV communications [7]. Finally, the effect of Doppler shift is assumed to be compensated in this work [1], [2].

Let the spatial location of the UAVs be uniformly distributed in a disc with radius r_a, angle $[0, 2\pi)$, and origin O above the FD-GS [5]. By letting the FD-GS be located on the ground at origin O, we define the Euclidean distance (in km) between UL UAV-i and the FD-GS as $d_{i,g} = \sqrt{D^2_{i,g} + \left(D^{UL}_{alt,i} + \lambda_{i,g}\right)^2}$, where $D_{i,g}$ denotes the Euclidean distance between the projection of UL UAV-i onto the ground plane and the FD-GS. Similarly, let the Euclidean distance between the FD-GS and DL UAV be $d_{g,1} = \sqrt{D^2_{g,1} + \left(D^{DL}_{alt,1} + \lambda_{g,1}\right)^2}$, where $D_{g,1}$ denotes the Euclidean distance between the projection of the DL UAV onto the ground plane and the FD-GS. The variable λ_x, $x \in \{(i,g),(g,1)\}$ denotes a minimum distance between the UAVs and the FD-GS such that $0 < \lambda_x < r_a$, $D^{UL}_{alt,i} \leq D^{UL}_{alt,i+1}$ and $\lambda_{i,g} < \lambda_{i+1,g}$, are satisfied to enable the SIC-based detection process at the FD-GS. Finally, we define the Euclidean distance between the UL and DL UAVs, i.e., inter-UAV distance, as $d_{i,1}$.

As the spatial locations of the UAVs follow a BPP, the probability density function (PDF) $f_{d_x}(w)$ of d_x is defined as [5, eq. (3)] $f_{d_x}(w) = \frac{2w}{r_a^2}$ where $x \in \{(i,g),(g,1)\}$, $D_{alt} + \lambda_x \leq w \leq \sqrt{\left(D_{alt} + \lambda_x\right)^2 + r_a^2}$, and $D_{alt} \in \{D_{alt,i}^{UL}, D_{alt,1}^{DL}\}$.

For the inter-UAV distance ($d_{i,1}$), the conditional PDF $f_{d_{i,1}}(w|d_{g,1})$ is given as [5, eq. (2)]:

$$f_{d_{i,1}}(w|d_{g,1}) = \begin{cases} \frac{2w}{r_a^2}, & \lambda_{i,1} \leq w \leq w_{m,1} \\ \frac{2w}{\pi r_a^2} \arccos\left(\frac{w^2 + d_{g,1}^2 - (r_a^2 + \lambda_{i,1}^2)}{2d_{g,1}\sqrt{w^2 - \lambda_{i,1}^2}}\right), & w_{m,1} < w \leq w_{p,1} \end{cases} \quad (1)$$

where $w_{m,1} = \sqrt{(r_a - d_{g,1})^2 + (\lambda_{i,1})^2}$, $w_{p,1} = \sqrt{(r_a + d_{g,1})^2 + (\lambda_{i,1})^2}$, and $0 < \lambda_{i,1} < w_{m,1}$ is the minimum distance between UL UAV-i and the DL UAV.

At the FD-GS, only residual SI is considered, with the SI channel modeled as a Rician fading channel to account for SI mitigation [1], [2]. Let x_{gs} and x_i be the respective transmitted signals from the FD-GS and UL UAV-i. Then, the signal-of-interest (SOI) and the SI signal at the FD-GS are x_i and $x_{si} = x_{gs}$, respectively. Also, let $h_{i,g}$ denote the channel between UL UAV-i and GS, and h_{si} be the SI channel gain. The resultant received signal at GS can thus be written as [3] $y_{gs} = \sum_{i=1}^{N_{UL}} \sqrt{\frac{P_i}{d_{i,g}^n}} h_{i,g} x_i + \sqrt{P_{si}} |\widetilde{h}_{si}| x_{si} + \sqrt{P_{si}} |h_{si}| \gamma_\phi w_\phi + w_g$, where n is the pathloss exponent, P_i is the transmit power of UL UAV-i, P_{si} is the power of the SI, $\widetilde{h}_{si}$ is the error of the imperfect SI channel gain estimate, defined as $\widetilde{h}_{si} = h_{si} - \widehat{h}_{si}$, $\widehat{h}_{si}$ is the imperfect estimation of the SI channel gain, w_g is the additive white Gaussian noise (AWGN) with zero-mean and variance σ_g^2, and w_ϕ is the Gaussian distributed phase noise with zero-mean and unit variance scaled by the strength of the phase noise γ_ϕ^2 [3]. [2]

To model the worst case residual SI, the channel estimation error ($\widetilde{h}_{si}$) is modeled as a circularly symmetric zero-mean complex Gaussian random variable (RV) with variance ϵ [1], [2]. Also, the total amount of SI suppression is $\frac{1}{\epsilon \sigma_g^2}$ [2]. Finally, as $D_{alt,i}^{UL} \leq D_{alt,i+1}^{UL}$ and $\lambda_{i,g} < \lambda_{i+1,g}$, the SIC-based detection order begins from UL UAV-i at the FD-GS, i.e., closest UL UAV, while treating the remaining $N_{UL} - i$ UL UAVs as interference.

At the DL UAV, the received signal can be written as $y_{DL} = \sqrt{\frac{P_g}{d_{g,i}^n}} h_{g,1} x_{gs} + \sum_{j=1}^{N_{UL}} \sqrt{\frac{P_j}{d_{j,1}^n}} h_{j,1} x_j + w_1$, where P_g is the transmit power of the GS, $h_{g,1}$ is the channel between the FD-GS and the DL UAV, $h_{j,1}$ is the channel between UL UAV-j and the DL UAV, and w_1 is the AWGN at the DL UAV with zero-mean and variance σ_1^2. As inter-UAV interference (x_i) is present at the DL UAV, we consider an imperfect SIC detector which removes inter-UAV interference first before detecting the SOI (x_{gs}).

III. Outage Probability

In this section, outage probability expressions of the UL and DL UAVs are presented for the HBD-UCS. The outage probability expression for HD-UCS is also presented for benchmark comparison. Let R_i^j and R_{gs}^j for $j \in \{HBD, HD\}$ be the transmission rates of the UL UAV-i and GS, respectively. For a fair comparison between the HBD-UCS and HD-UCS, we let $R_i^{HBD} = \frac{1}{2N_{UL}} R_i^{HD}$ and $R_{gs}^{HBD} = \frac{1}{2} R_{gs}^{HD}$ for uplink and downlink transmissions, respectively.

A. Hybrid-Duplex Outage Probability

For a SINR of $\frac{X_i d_i^{-n}}{1 + \sum_{j=i+1}^{N} X_j d_j^{-n}}$ with N interferers, where $X_i, 0 \leq i \leq N$ is a non-centered Chi-squared distributed random variable (RV) with Rician K factor K_i, and d_l^{-n} denotes the distance of transmitting node l, the outage probability is presented in the following Lemma.

Lemma 1: The outage probability $Pr(O)$ for the outage event O at an arbitrary receiver is:

$$\begin{aligned} Pr(O) \approx & \sum_{q=0}^{K_{tr}} \sum_{l_1 + \ldots + l_{N-q+1} = q+1} \alpha(q, \overline{P}_i, K_i, \gamma) \\ & \times \binom{l_1 + \ldots + l_{N-q+1}}{l_1, \ldots, l_{N-q+1}} \int_{-\infty}^{\infty} w_i^{n(q+1)} f_{d_i}(w_i) \\ & \times \left(\prod_{j=1}^{N-i} E\left\{X_j^{l_j}\right\} \int_{-\infty}^{\infty} w_j^{-nl_j} f_{d_j}(w_j) dw_j \right) dw_i, \quad (2) \end{aligned}$$

where $O = \left\{X_i, X_j : R \geq \log_2\left(1 + \frac{X_i d_i^{-n}}{1 + \sum_{j=i+1}^{N} X_j d_j^{-n}}\right)\right\}$, R is the transmission rate, K_{tr} is the truncation order, $\alpha(q, \overline{P}_i, K_i, \gamma) = (-1)^q \exp(-K_i) \frac{L_q^{(i)}(K_i)}{(1+q)!} \left(\frac{(1+K_i)}{\overline{P}_i}\gamma\right)^{q+1}$ is the cumulative distribution function (CDF) expansion of the RV X_i, $\overline{P}_i$ is the variance of X_i, γ is the threshold, $L_q^{(0)}(\bullet)$ is the q-th degree, zero-order Laguerre polynomials [1], [2], and $E\{\bullet\}$ is the statistical expectation. Also, $E\left\{X_j^{l_j}\right\} = \Gamma(1 + l_j) \left[\frac{\overline{P}_j}{1+K_j}\right]^{l_j} {}_1F_1(-l_j, 1; -K_j)$ is the l_j^{th} moment of X_j [2, eq. (7)] with ${}_1F_1(\bullet)$ representing the confluent Hypergeometric function [2].

Proof: The proof is provided in Appendix A. ∎

From Lemma 1, the outage probability expressions of the UL and DL UAVs can be obtained.

1) Uplink UAV-i: Let $X_{i,g} = P_{i,g}|h_{i,g}|^2$ be the instantaneous received power of the SOI from UL UAV-i at the FD-GS, where $P_{i,g} = \frac{P_i}{\sigma_g^2}$. Also, let $Y_{si,1} = P_{si}\gamma_\phi^2 |h_{si}|^2$ and $Y_{si,2} = P_{si}\epsilon|\widetilde{h}_{si}|^2$ be the instantaneous received power of the residual SI components, where $P_{si} = P_{i,g}$. The symbols $X_{i,g}$ and $Y_{si,1}$ are non-centered Chi-squared distributed RVs with respective Rician K factors $K_{i,g}$ and $K_{si,1}$ while $Y_{si,2}$ is an exponentially distributed RV. Defining the outage event of UL UAV-i as $O_{UL,i}^{HBD} = \left\{h_{i,g}, h_{si} : R_i^{HBD} \geq \log_2\left(1 + \frac{X_{i,g} d_{i,g}^{-n}}{\sum_{j=i+1}^{N_{UL}} X_{j,g} d_{j,g}^{-n} + Y_{si,1} + Y_{si,2} + 1}\right)\right\}$, with threshold $\gamma_{gs}^{HBD} = 2^{R_i^{HBD}} - 1$, the outage probability $Pr(O_{UL,i}^{HBD})$ of UL UAV-i is presented in the following theorem:

Theorem 1: The outage probability at UL UAV-i is

$$\begin{aligned} Pr(O_{UL,i}^{HBD}) \approx & \sum_{q=0}^{K_{tr}} \sum_{l_1 + \ldots + l_{N_{UL}-i+3} = q+1} \alpha(q, P_{i,g}, K_{i,g}, \gamma_{gs}^{HBD}) \\ & \times \Delta(D_{alt,i}^{UL}, \lambda_{i,g}, q) \binom{l_1 + \ldots + l_{N_{UL}-i+3}}{l_1, \ldots, l_{N_{UL}-i+3}} E\left\{Y_{si,1}^{l_1}\right\} E\left\{Y_{si,2}^{l_2}\right\} \end{aligned}$$

[2]The phase noise term γ_ϕ reflects the jitter effect in oscillators due to hardware imperfections [3]

$$\times \prod_{j=1}^{N_{UL}-i} E\left\{X_{j,g}^{l_j}\right\} \overline{\Delta}\left(D_{alt,j}^{UL}, \lambda_{j,g}, l_j\right), \quad (3)$$

where $n \neq 2$, $\Delta\left(D_{alt,i}^{UL}, \lambda_{i,g}, q\right) = \frac{2}{[n(q+1)+2]r_a^2}\left(\left[\left(D_{alt,i}^{UL}+\lambda_{i,g}\right)^2 + r_a^2\right]^{\frac{n(q+1)+2}{2}} - \left[\left(D_{alt,i}^{UL}+\lambda_{i,g}\right)^2\right]^{\frac{n(q+1)+2}{2}}\right)$, and $\overline{\Delta}\left(D_{alt,j}^{UL}, \lambda_{j,g}, l_j\right) = \frac{2}{[2-nl_j]r_a^2}\left(\left[\left(D_{alt,j}^{UL}+\lambda_{j,g}\right)^2 + r_a^2\right]^{\frac{2-nl_j}{2}} - \left[\left(D_{alt,j}^{UL}+\lambda_{j,g}\right)^2\right]^{\frac{2-nl_j}{2}}\right)$.

Proof: Applying Lemma 1 and integrating the resulting expression over the PDFs $f_{d_{i,g}}(w_i)$ and $f_{d_{j,g}}(w_j)$ yields Theorem 1. ∎

As $2-nl_j$ is present in the denominator of $\overline{\Delta}\left(D_{alt,j}^{UL}, \lambda_{j,g}, l_j\right)$, Theorem 1 is valid only when $n \neq 2$. However, it must be noted that selecting $n \approx 2$, e.g., $n = 2 + 10^{-6}$, enables Theorem 1 to be applied for outage probability analysis involving free space path loss scenarios. [3]

2) Downlink UAV: At the DL UAV, let $X_{g,1} = P_{g,1}|h_{g,1}|^2$ be the instantaneous received power of the SOI from the GS at the DL UAV, where $P_{g,1} = \frac{P_g}{\sigma_1^2}$. Also, let $X_{j,1} = P_{j,1}\beta_{j,1}|h_{j,1}|^2$ be the instantaneous received powers of the inter-UAV interference from UL UAV-j due to HBD transmissions, where $P_{j,1} = \frac{P_j}{\sigma_1^2}$, and $0 \leq \beta_{j,1} \leq 1$ denotes the strength of the residual interference due to imperfect SIC. The symbols $X_{g,1}$ and $X_{j,1}$ are non-centered Chi-squared distributed RVs with respective Rician K factors $K_{g,1}$ and $K_{j,1}$. Defining the outage event at the DL UAV as $O_{DL}^{HBD} = \left\{h_{g,1}, h_{j,1} : R_{gs}^{HBD} \geq \log_2\left(1 + \frac{X_{g,1}d_{g,1}^{-n}}{\sum_{j=1}^{N_{UL}} X_{j,1}d_{j,1}^{-n}+1}\right)\right\}$, the outage probability expression for the DL UAV is presented in the following theorem.

Theorem 2: The HBD outage probability at the DL UAV is

$$Pr\left(O_{DL}^{HBD}\right) \approx \sum_{q=0}^{K_{tr}} \sum_{l_1+\ldots+l_{N_UL+1}=q+1} \alpha\left(q, P_{g,1}, K_{g,1}, \gamma_{DL}^{HBD}\right) \times \binom{l_1+\ldots+l_{N_UL-i+3}}{l_1,\ldots,l_{N_UL-i+3}} \int_{L_1}^{L_2} \frac{2w_{g,1}^{n(q+1)+1}}{r_a^2} \times \left(\prod_{j=1}^{N_{UL}} E\left\{X_{j,1}^{l_j}\right\} \Xi_{j,1}(w_{g,1}, l_j)\right) dw_{g,1}, \quad (4)$$

where $L_1 = D_{alt,1}^{DL} + \lambda_{g,1}$, $L_2 = \sqrt{\left(D_{alt,1}^{DL}+\lambda_{g,1}\right)^2 + r_a^2}$, $\gamma_{DL}^{HBD} = 2^{R_{gs}^{HBD}} - 1$, and $\Xi_{j,1}(w_{g,1}, l_j) = \frac{2\left[(w_{m,1})^{2-nl_j} - \lambda_{j,1}^{2-nl_j}\right]}{r_a^2[2-nl_j]} + \int_{w_{m,1}}^{w_{p,1}} \frac{2w_{j,1}}{\pi r_a^2} \arccos\left(\frac{w_{j,1}^2+w_{g,1}^2-(r_a^2+\lambda_{j,1}^2)}{2w_{g,1}\sqrt{w_{j,1}^2-\lambda_{j,1}^2}}\right) dw_{j,1}$.

Proof: Theorem 2 is proven using the same approach in Theorem 1. ∎

B. Half-Duplex Outage Probability

We compare the HBD-UCS with HD-UCS as a benchmark scheme. For the HD-UCS, an outage is declared for UL UAV-i when $R_i^{HD} \geq \log_2\left(1 + X_{i,g}d_{i,g}^{-n}\right)$. Similarly, an outage is declared for the DL UAV when $R_{gs}^{HD} \geq \log_2\left(1 + X_{g,1}d_{g,1}^{-n}\right)$. Thus, the HD-UCS outage events for UL UAV-i and the DL UAV are defined as $O_{UL,i}^{HD} = \left\{h_{i,g} : R_i^{HD} \geq \log_2\left(1+X_{i,g}d_{i,g}^{-n}\right)\right\}$ and $O_{DL}^{HD} = \left\{h_{g,1} : R_{gs}^{HD} \geq \log_2\left(1 + X_{g,1}d_{g,1}^{-n}\right)\right\}$, respectively. Following the same approach presented in Appendix A, the HD-UCS outage probability expressions for UL UAV-i and the DL UAV are:

$$Pr\left(O_{UL,i}^{HD}\right) \approx \sum_{q=0}^{K_{tr}} \alpha\left(q, P_{i,g}, K_{i,g}, \gamma_{gs}^{HD}\right)\Delta\left(D_{alt,i}^{UL}, \lambda_{i,g}, q\right), \quad (5)$$

$$Pr\left(O_{DL}^{HD}\right) \approx \sum_{q=0}^{K_{tr}} \alpha\left(q, P_{g,1}, K_{g,1}, \gamma_{DL}^{HD}\right)\Delta\left(D_{alt,1}^{DL}, \lambda_{g,1}, q\right), \quad (6)$$

where $\gamma_{gs}^{HD} = 2^{R_1^{HD}} - 1$ and $\gamma_{DL}^{HD} = 2^{R_{gs}^{HD}} - 1$.

IV. Numerical Results

The outage probability of the HBD-UCS is analyzed in this section for Rician K factors of 10 dB [7, Table V], 0 dB $\leq P_t \leq$ 30 dB, $P_{i,g} = P_{g,1} = P_{j,1} = P_t$, $\sigma_g^2 = \sigma_1^2 = -131$dBm [8], $R_x^{HD} = 0.1$b/s/Hz, $i \in \{i, gs\}$, $\gamma_\phi^2 = -140$dBm, $\epsilon = 0.01$ [2], $r_a = 4$ km, $n \approx 2$ [7, Table III], $N_{UL} = 3$, $\lambda_{1,g} = 1.3$, $\lambda_{2,g} = 1.4$, $\lambda_{3,g} = 1.5$, $\beta_{j,1} = 0.5^2$, and Monte Carlo simulations using 10^5 samples.

The outage probability of the HBD-UCS is compared against the HD-UCS for both UL and DL transmissions in Fig. 2. At low P_t regimes, the HBD-UCS outperforms the HD-UCS in terms of UL and DL outage probability. In particular, the HBD-UCS is able to fulfill packet error rate (PER) requirements for UAV control links over Long Term Evolution (LTE) networks, i.e., $PER < 10^{-3}$ [9]. [4] Additionally, for UL transmissions, recall that the FD-GS detects UL UAV-i by treating the remaining $N_{UL} - i$ UL UAVs as interference. As such, UL UAV-1 is seen to exhibit higher outage probability than UL UAV-2 and UAV-3, with similar observations also noted for the subsequent UL UAVs. It is also seen that, depending on the number of interfering UL UAVs, the DL UAV can also attain lower DL outage probability than the HD-UCS at moderate P_t regimes, e.g., $N_{UL} \in \{2, 3\}$.

At high P_t regimes, the HD-UCS attains lower outage probability than the HBD-UCS for both UL and DL outage probability. For UL transmissions, error floors are observed since the detection process at the FD-GS becomes interference-limited due to interference from the remaining $N_{UL} - i$ UL UAVs. Similarly, for DL transmissions, error floors are observed due to the DL UAV becoming interference-limited as a result of residual SIC interference. Thus, it is shown that the HBD-UCS is well suited for multi-UAV networks since UAV

[3] Selecting $n \approx 2$, e.g., $n = 2 + 10^{-6}$, allows $\overline{\Delta}\left(D_{alt,j}^{UL}, \lambda_{j,g}, l_j\right)$ to be evaluated for free space path loss scenarios while avoiding a zero in the denominator.

[4] Outage probability can be used to represent PER if the transmitted signals span over one fading block [2].

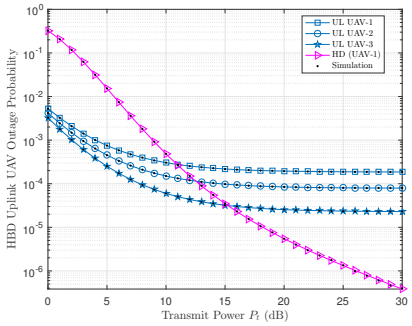

(a) Uplink outage probability.

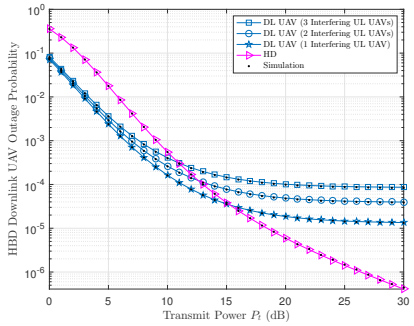

(b) Downlink outage probability for $\lambda_{1,1} = 1.4$, $\lambda_{2,1} = 1.3$, and $\lambda_{3,1} = 1.2$.

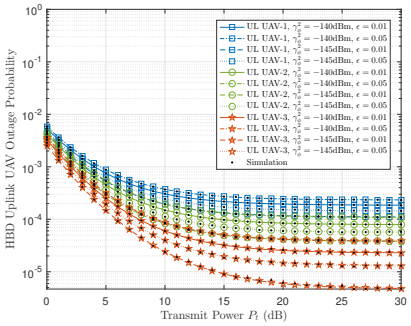

(c) Impact of SI cancellation and phase noise on uplink outage probability.

Fig. 2. Outage probability of the HBD-UCS.

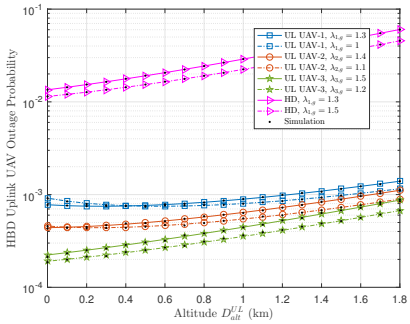

(a) Uplink outage probability.

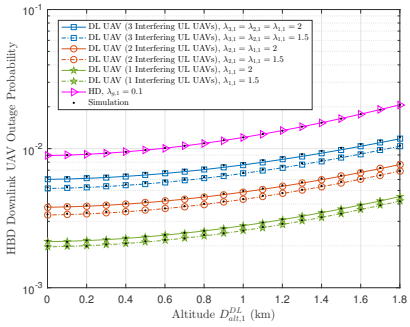

(b) Downlink outage probability.

Fig. 3. Impact of height and minimum distance on the outage probability of the HBD-UCS at $P_t = 5$ dB, $\beta = 1$, $\lambda_{g,1} = 0.1$, and $D_{alt}^{UL} = D_{alt,i}^{UL}$.

communications operate at low P_t regimes. [5] [6] The impact of SI cancellation and phase noise on uplink outage probability is seen in Fig. 2c. It is observed that an increase in either γ_ϕ^2 or ϵ causes the outage probability of the UL UAVs to increase. Furthermore, an increasing γ_ϕ^2 causes higher outage probability than an increasing ϵ due to higher residual SI at the FD-GS. Thus, the reliability of UL UAV transmissions in an HBD-UCS hinges on having effective SI mitigation architectures with low phase noise FD transceivers at the GS.

In Fig. 3, the impact of height and minimum distance on the outage probability of the HBD-UCS is analyzed. For UL transmissions, a lower outage probability is attained when $0 \leq D_{alt}^{UL} \leq 1$ and $\lambda_{i,g}$ is reduced, since weaker UL interference is experienced. However, when $D_{alt}^{UL} > 1$, outage probability increases due to a weaker SOI. Similarly, increasing $\lambda_{i,g}$ leads to higher outage probability as the SOI is further weakened. For DL transmissions, increasing $D_{alt,1}^{DL}$ leads to higher outage probability for the HBD-UCS and HD-UCS due to a weaker SOI. It is also observed that increasing $\lambda_{i,1}$ reduces outage probability since inter-UAV interference is weakened. Therefore, as seen in Fig. 3, one may have to consider other approaches if support for UAVs deployed at high altitudes is required. Nonetheless, Fig. 2 and Fig. 3 have demonstrated that the multi-UAV network with HBD-UCS is able to support more UAVs concurrently on the same spectrum while attaining a lower outage probability than the HD-UCS.

V. Conclusion

In this paper, the outage probability analysis of a multi-UAV network with HBD-UCS is investigated within a stochastic geometry framework. It is demonstrated that at low transmit power regimes, the HBD-UCS achieves lower outage probability than the HD-UCS for both uplink and downlink transmissions. It is also shown that the HBD-UCS can support uplink and downlink transmissions that are more reliable than the HD-UCS, when the UAV operating altitude is increased. Thus, we demonstrate that the HBD-UCS is able to concurrently support more UAVs while achieving a higher reliability than the HD-UCS.

Appendix A
Proof of Lemma 1

From [2, eq. (6)], the conditional outage probability $Pr(O|d_i, d_j)$ at receiver i is $Pr(O|d_i, d_j) \approx \sum_{q=0}^{K_{tr}} \sum_{l_1+\ldots+l_{N-i+1}=q+1} \alpha\left(q, \overline{P}_i d_i^{-n}, K_i, \gamma\right) \binom{l_1+\ldots+l_{N-i+1}}{l_1,\ldots,l_{N-i+1}} \prod_{j=1}^{N-i} E\left\{\left(X_j d_j^{-n}\right)^{l_j}\right\}$. Thereafter, averaging $Pr(O|d_i, d_j)$ over the respective distributions of d_i and d_j yields Lemma 1. This completes the proof.

References

[1] T. Z. H. Ernest, A. Madhukumar, R. P. Sirigina, and A. K. Krishna, "A Hybrid-Duplex System with Joint Detection for Interference-Limited UAV Communications," *IEEE Trans Veh. Technol.*, Jan. 2019.

[5] It is worth noting that UAVs largely operate at low P_t regimes due to size, weight, and power restrictions. For instance, 29dBm $\leq P_t \leq$ 40dBm was noted in [8], while in [10], cellular-to-UAV links were evaluated for $P_t = 20$dBm. The values found in [8], [10] translates into -10dB $\leq P_t \leq$ 10dB.

[6] Outage probability can be further reduced when the transmit power and trajectory of the UAVs are optimized iteratively. For transmit power optimization, one should consider the spatial location of the UAVs and the trajectory. For trajectory optimization, both the spiral and oval trajectory processes should be considered to maintain a uniform distribution under the BPP model [11].

[2] ——, "Outage Analysis and Finite SNR Diversity-Multiplexing Tradeoff of Hybrid-Duplex Systems for Aeronautical Communications," *IEEE Trans Wireless Commun.*, April 2019.
[3] A. Sahai, G. Patel, C. Dick, and A. Sabharwal, "On the impact of phase noise on active cancelation in wireless full-duplex," *IEEE Trans. Veh. Technol*, vol. 62, no. 9, pp. 4494–4510, 2013.
[4] Z. Wei, S. Sun, X. Zhu, Y. Huang, and J. Wang, "Energy-efficient hybrid duplexing strategy for bidirectional distributed antenna systems," *IEEE Trans. Veh. Technol.*, vol. 67, no. 6, pp. 5096–5110, 2018.
[5] V. V. Chetlur and H. S. Dhillon, "Downlink coverage analysis for a finite 3-d wireless network of unmanned aerial vehicles," *IEEE Trans. Commun*, vol. 65, no. 10, pp. 4543–4558, 2017.
[6] X. Wang, H. Zhang, Y. Tian, and V. C. Leung, "Modeling and analysis of aerial base station-assisted cellular networks in finite areas under los and nlos propagation," *IEEE Trans. Wireless Commun.*, vol. 17, no. 10, pp. 6985–7000, October 2018.
[7] D. W. Matolak and R. Sun, "Air-ground channel characterization for unmanned aircraft systems part iii: The suburban and near-urban environments," *IEEE Trans. Veh. Technol*, 2017.
[8] ITU, "Itu-r report m.2233, examples of technical characteristics for unmanned aircraft control and nonpayload communications links," Tech. Rep., 2011.
[9] 3GPP TR36.77, "Study on Enhanced LTE Support for Aerial Vehicles," Tech. Rep., 2017.
[10] Y. Zeng, J. Lyu, and R. Zhang, "Cellular-connected uav: Potential, challenges and promising technologies," *IEEE Wireless Commun.*, pp. 1–8, 2018.
[11] S. Enayati, H. Saeedi, H. Pishro-Nik, and H. Yanikomeroglu, "Moving aerial base station networks: Stochastic geometry analysis and design perspective," *IEEE Trans. Wireless Commun.*, 2019.